RESEARCH ARTICLE • OPEN ACCESS

Parameter Estimation of a Climate-Based Dengue Mathematical Model in Bandung City Using the Particle Swarm Optimization Algorithm

Sindi Meli Nur Afni, Khusnul Novianingsih, and Ririn Sispiyati

JAMBURA JOURNAL OF MATHEMATICS

Volume 8, Issue 2, Pages 242–256, August 2026

Received 25 May 2026, Revised 7 August 2026, Accepted 11 August 2026, Published 17 August 2026

To Cite this Article : S. M. N. Afni, K. Novianingsih, and R. Sispiyati,"Parameter Estimation of a Climate-Based Dengue Mathematical Model in Bandung City Using the Particle Swarm Optimization Algorithm", *Jambura J. Math*, vol. 8, no. 2, pp. 242–256, 2026, *https://doi.org/10.37905/jjom.v8i2.39153*

JOURNAL INFO • JAMBURA JOURNAL OF MATHEMATICS

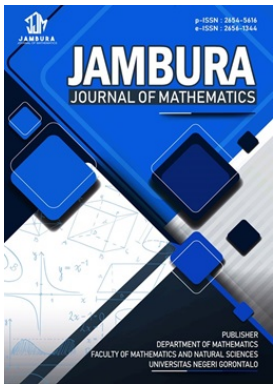

Homepage	:	http://ejurnal.ung.ac.id/index.php/jjom/index
Journal Abbreviation	:	Jambura J. Math.
Frequency	:	Biannual (February and August)
Publication Language	:	English (preferable), Indonesia
DOI	:	https://doi.org/10.37905/jjom
Online ISSN	:	2656-1344
Editor-in-Chief	:	Hasan S. Panigoro
Publisher	:	Department of Mathematics, Universitas Negeri Gorontalo
Country	:	Indonesia
OAI Address	:	http://ejurnal.ung.ac.id/index.php/jjom/oai
Google Scholar ID	:	iWLjgaUAAAAJ
Email	:	info.jjom@ung.ac.id

JAMBURA JOURNAL • FIND OUR OTHER JOURNALS

Jambura Journal of Biomathematics

Jambura Journal of Mathematics Education

Jambura Journal of Probability and Statistics

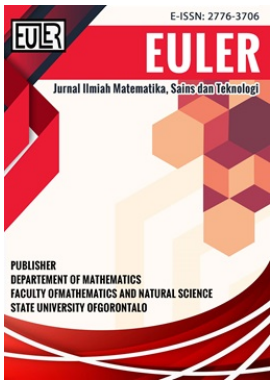

EULER : Jurnal Ilmiah Matematika, Sains, dan Teknologi

Jambura Journal of Mathematics, Volume 8, Issue 2, Pages 242–256, August 2026 https://doi.org/10.37905/jjom.v8i2.39153

Research Article

Check for updates

Parameter Estimation of a Climate-Based Dengue Mathematical Model in Bandung City Using the Particle Swarm Optimization Algorithm

Sindi Meli Nur Afni[1], **Khusnul Novianingsih**[1,*], **Ririn Sispiyati**[1]

[1]*Department of Mathematics, Universitas Pendidikan Indonesia, Bandung, 40154, Indonesia*

ARTICLE HISTORY
Received 25 May 2026
Revised 7 August 2026
Accepted 11 August 2026
Published 17 August 2026

KEYWORDS
Dengue Hemorrhagic Fever
SEIR Model
Parameter Estimation
Particle Swarm Optimization
MAPE

ABSTRACT. *Dengue Hemorrhagic Fever (DHF) is spread through the bite of the Aedes aegypti mosquito and is affected by the environment, especially temperature and rainfall. The purpose of this study is to create a SEIR (Susceptible–Exposed–Infected–Recovered) mathematical model taking into account the effects of climate factors and to estimate the parameters of this model using the Particle Swarm Optimization (PSO) algorithm. The analyzed data consisted of monthly reports of the number of dengue fever cases, temperature, and rainfall for the city of Bandung in 2022–2023 and were smoothed using a moving average. The parameter estimation process was performed by minimizing the Mean Absolute Percentage Error (MAPE), and the numerical simulation of the model was performed using the fourth-order Runge–Kutta method (RK4). The results of this study show that the model has two equilibrium points: a disease-free equilibrium point and an endemic equilibrium point, and the stability of the equilibrium points depends on the basic reproduction number R_0. The best parameters obtained were $\beta_0 = 3.5553$, $\beta_1 = 0.0021$, $\beta_2 = 0.0001$, $\sigma = 7.5$, $\mu = 0.0011$, and $\gamma = 3.6865$, with an MAPE value of 0.1740 or 17.40%. These findings indicate that the model is able to represent the pattern of dengue fever spread with a low level of prediction error. Sensitivity analysis showed that the recovery rate parameter (γ) was the most responsive to changes in the model.*

1. Introduction

Dengue Hemorrhagic Fever (DHF) is one of the tropical diseases that remains a major global public health problem. The disease is caused by the dengue virus, which is transmitted through the bites of Aedes aegypti and Aedes albopictus mosquitoes, both of which are active during the daytime and commonly breed in urban environments [1]. Dengue is one of the fastest-growing mosquito-borne diseases worldwide, with more than 14.1 million cases recorded in 2024, representing a significant increase compared with the previous year [2]. In Indonesia, dengue remains a serious public health problem because of its high incidence and frequent outbreaks. In Bandung, the number of DHF cases reached 1,653 from January to June 2025, the highest number reported in West Java. This figure indicates that existing control measures remain insufficiently effective, with environmental factors and increasing mosquito populations being among the main contributing factors [3]. Therefore, it is important to apply mathematical modelling techniques that incorporate climatic factors to describe dengue transmission more accurately and support appropriate decision-making for disease control.

In the model development process, several parameters determine the accuracy of the model. These parameters include the disease transmission rate, incubation rate, recovery rate, mortality rate, and coefficients representing the effects of climatic factors such as temperature, rainfall, and humidity on vector-related parameters [4]. A mathematical model cannot be reliably applied to real-world conditions if the values of its parameters are unknown [5]. Therefore, parameter estimation is crucial because it directly affects the accuracy of the model used to predict dengue transmission. Consequently, appropriate parameter estimation needs to be performed [6].

Several studies have developed mathematical models to investigate dengue transmission. Mathematical epidemic modelling has commonly employed compartmental approaches that divide the population into Susceptible (S), Exposed (E), Infected (I), and Recovered (R) compartments. However, many existing models remain limited in their representation of local environmental conditions. Several studies have focused primarily on biological aspects without incorporating local climatic factors that significantly influence dengue dynamics [7]. In particular, climatic variables such as temperature and rainfall are often not comprehensively considered, even though they can have substantial effects on dengue transmission [8]. Climatic factors strongly influence the growth dynamics and population size of Aedes aegypti mosquitoes, which are the primary vectors of dengue. Increasing temperature can accelerate the development of eggs, larvae, and pupae into adult mosquitoes, shorten the development of dengue virus within the mosquito, and increase mosquito biting frequency [9]. Meanwhile, rainfall can create additional breeding sites in the form of standing water, thereby increasing mosquito populations [10]. Together, these climatic factors may increase the likelihood of dengue transmission. Therefore, climatic variables should be integrated into epidemiological models so that dengue transmission dynamics can

*Corresponding Author.

Email : *k_novianingsih@upi.edu* (K. Novianingsih)
Homepage : http://ejurnal.ung.ac.id/index.php/jjom/index / E-ISSN : 2656-1344

be represented more accurately and realistically [11].

In addition, parameter estimation methods applied in previous studies have generally relied on classical approaches, such as Maximum Likelihood Estimation (MLE) [12] and Bayesian MCMC [13]. These classical methods have several limitations when applied to nonlinear epidemic models involving multiple variables. MLE requires an accurately specified likelihood function and may be vulnerable to parameter identifiability problems, which can lead to non-unique parameter estimates in complex epidemic models [14]. On the other hand, Bayesian MCMC requires a large number of simulations, resulting in high computational costs, while its convergence depends on the selection of prior distributions and appropriate Markov chain diagnostics [15]. Therefore, epidemic models with nonlinear objective functions and complex parameter spaces require optimization methods capable of performing efficient global searches without depending on the explicit form of a likelihood function. Furthermore, research on the use of metaheuristic methods for this parameter estimation problem remains limited. Metaheuristic methods have advantages in solving nonlinear optimization problems with complex search spaces because they are capable of performing global searches and reducing the possibility of becoming trapped in local optima [16].

To date, Genetic Algorithm (GA) [17] and Particle Swarm Optimization (PSO) [18] have been applied to parameter estimation problems. However, these studies did not incorporate climatic variables. This study addresses this research gap by applying parameter estimation to a climate-based SEIR model using PSO. PSO was selected as the estimation method because it has been shown to be efficient and adaptive, with favorable stability and global convergence properties [19]. The climatic variables incorporated in this study are temperature and rainfall. The data used consist of dengue cases in Bandung City during 2022–2023.

Accurate parameter estimation plays an important role in epidemiological analysis. This study employs an SEIR model with a reduced-model approach for the human population. This approach differs from previous studies that generally applied disease models without explicitly incorporating environmental factors. In the proposed model, changes in the mosquito population are not represented as a separate compartment but are incorporated through an effective transmission rate $\beta(T, P)$ that is directly influenced by climatic variables, namely temperature and rainfall.

The time-lag effect of climate on vector biology is not explicitly included in the model because the direct use of the effective transmission rate $\beta(T, P)$ allows climatic effects to be represented continuously and efficiently [20], without increasing the complexity of a delay differential equation (DDE) system that may potentially lead to overfitting during parameter optimization. This approach is therefore expected to provide a more efficient and accurate framework for parameter estimation using the PSO algorithm.

2. Model

2.1. Model and Assumptions

The model applied in this study is the SEIR (Susceptible–Exposed–Infected–Recovered) model. The effects of temperature and rainfall are incorporated into the transmission rate parameter $\beta(T, P)$ because both factors influence the activity of Aedes aegypti, the primary vector of Dengue Hemorrhagic Fever (DHF). The model does not explicitly describe changes in the mosquito population or account for the time lag between climatic effects and the biological response of the vector. Instead, the direct use of the effective transmission rate $\beta(T, P)$ allows climatic effects to be incorporated continuously and efficiently. The SEIR model is then analyzed for Bandung City using a parameter estimation method based on the Particle Swarm Optimization (PSO) algorithm. The changes in the number of individuals in each compartment of the SEIR model, including the effects of temperature and rainfall, are represented as follows.

2.1.1. Susceptible Compartment (S)

The number of individuals in the Susceptible compartment increases through new births at a rate Λ. By applying the constant population condition $\Lambda = \mu N$, the number of births is balanced with the total natural mortality rate of the population. The number of individuals in this compartment decreases due to natural mortality at a rate μS and disease transmission from infected individuals at a rate $\beta(T, P)SI/N$. Therefore, the rate of change of the susceptible population with respect to time is expressed as

$$\frac{dS}{dt} = \Lambda - \beta(T, P)\frac{SI}{N} - \mu S, \tag{1}$$

where the condition $\Lambda = \mu N$ is applied.

2.1.2. Exposed Compartment (E)

Individuals enter the Exposed compartment from the susceptible population through infection at a rate $\beta(T, P)SI/N$. Meanwhile, the number of individuals in the Exposed compartment decreases because individuals complete the incubation period and move to the Infected compartment at a rate σE, as well as through natural mortality at a rate μE. Therefore, the rate of change of the number of exposed individuals is

$$\frac{dE}{dt} = \beta(T, P)\frac{SI}{N} - (\sigma + \mu)E. \tag{2}$$

2.1.3. Infected Compartment (I)

Individuals entering the Infected compartment originate from exposed individuals who have completed the incubation period at a rate σE. The number of individuals in this compartment decreases through recovery at a rate γI and natural mortality at a rate μI. Therefore, the rate of change of the infected population is expressed as

$$\frac{dI}{dt} = \sigma E - (\gamma + \mu)I. \tag{3}$$

2.1.4. Recovered Compartment (R)

Individuals enter the Recovered compartment through the recovery of infected individuals at a rate γI. The number of individuals in this compartment decreases due to natural mortality at a rate μR. Therefore, the rate of change of the recovered population with respect to time is expressed as

$$\frac{dR}{dt} = \gamma I - \mu R. \tag{4}$$

2.1.5. SEIR Model System

Based on eq. (1) to (4), the mathematical model can be expressed as the following system of differential equations describing the SEIR dynamics with the effects of temperature and rainfall:

$$\begin{aligned} \frac{dS}{dt} &= \Lambda - \beta(T,P)\frac{SI}{N} - \mu S, \\ \frac{dE}{dt} &= \beta(T,P)\frac{SI}{N} - (\sigma+\mu)E, \\ \frac{dI}{dt} &= \sigma E - (\gamma+\mu)I, \\ \frac{dR}{dt} &= \gamma I - \mu R. \end{aligned} \tag{5}$$

with the initial conditions

$$S(0) > 0, \qquad E(0) > 0, \qquad I(0) > 0, \qquad R(0) > 0.$$

The rate of change of the total population $N(t) = S(t) + E(t) + I(t) + R(t)$ with respect to time is obtained by summing all differential equations in the system:

$$\begin{aligned} \frac{dN}{dt} &= \frac{dS}{dt} + \frac{dE}{dt} + \frac{dI}{dt} + \frac{dR}{dt} \\ &= \Lambda - \mu S - \mu E - \mu I - \mu R \\ &= \Lambda - \mu(S + E + I + R) \\ &= \Lambda - \mu N. \end{aligned} \tag{6}$$

Since $\Lambda = \mu N$ is assumed, it follows that $\frac{dN}{dt} = 0$, which shows that the total population N remains constant over time.

2.1.6. Climate Effects on the Transmission Rate

In this study, a reduced human population model is used in which the mosquito vector compartment, Aedes aegypti, is not included as a separate compartment. Instead, the effects of vector density and activity are incorporated directly through the effective transmission rate $\beta(T, P)$ as a linear function of temperature T and rainfall P:

$$\beta(T,P) = \beta_0 + \beta_1 T + \beta_2 P. \tag{7}$$

The parameters β_0, β_1, and β_2 represent the sensitivity parameters of the transmission rate to temperature and rainfall. A first-order Taylor approximation is used to describe the primary effects of temperature and rainfall within the empirical observation range representing tropical conditions [21]. In addition to maintaining a simple mathematical structure and avoiding high computational costs, this approach also facilitates the interpretation of the sensitivity coefficients β_1 and β_2 and provides a higher level of parameter identifiability during the optimization process using the PSO algorithm [22].

Mathematically, because temperature $T(t)$ and rainfall $P(t)$ vary over time, the differential equation system in eq. (5) is nonautonomous. For qualitative analysis, including the determination of equilibrium points, the basic reproduction number R_0, and local stability analysis, this study uses the average temperature and rainfall values during the observation period, denoted by $\overline{T}$ and $\overline{P}$. Meanwhile, in the numerical simulations using RK4 and in the PSO parameter estimation process, the values of $T(t)$ and $P(t)$ are incorporated dynamically according to the monthly data. The SEIR mathematical model is represented by the diagram in Figure 1.

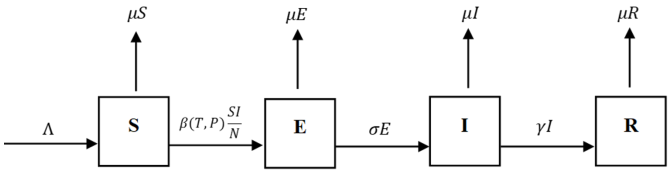

Figure 1. SEIR mathematical model diagram for Dengue Hemorrhagic Fever with the effects of temperature and rainfall.

The mathematical model is developed to investigate the transmission of DHF by considering the effects of temperature and rainfall. The assumptions of the model are as follows:

1. The human population is divided into four compartments: S (Susceptible), E (Exposed), I (Infected), and R (Recovered).
2. There is no movement of individuals into or out of the study area through immigration or emigration.
3. The number of new births is proportional to the total population at a rate $\Lambda = \mu N$, where the birth rate is balanced with the total natural mortality rate μN to maintain a constant total population size N over time.
4. Every individual, regardless of compartment, experiences natural mortality at the same rate μ.
5. Susceptible individuals S may become infected with the dengue virus through bites from infected mosquitoes at a transmission rate $\beta(T, P)SI/N$.
6. The transmission rate $\beta(T, P)$ depends on temperature T and rainfall P because these factors affect mosquito abundance, biting frequency, and dengue virus development.
7. Individuals entering the Exposed compartment have been infected with the virus but are not yet infectious because they are still in the incubation period.
8. Individuals move from the Exposed compartment to the Infected compartment at a rate σ, representing the rate at which the incubation period ends.
9. Individuals in the Infected compartment can transmit the virus and leave the compartment through recovery at a rate γ or through natural mortality at a rate μ.
10. Recovered individuals move to the Recovered compartment and are assumed to acquire temporary immunity against reinfection.
11. Individuals in the Recovered compartment may die naturally at a rate μ.
12. The total human population size N is assumed to remain constant throughout the observation period, with $N = S + E + I + R$. To maintain a constant population size under vital dynamics, the birth rate is assumed to balance the total natural mortality rate, so that $\Lambda = \mu N$.
13. For equilibrium point and R_0 analyses, climatic factors are assumed to remain constant at their average values, whereas in numerical simulations, climatic factors vary according to the monthly data.
14. The DHF case data were obtained from the Bandung City Health Office, while temperature and rainfall data were obtained from Statistics Indonesia (BPS) of Bandung City.

Table 1. List of variables in the SEIR model.

No.	Variable	Definition	Condition	Unit
1	$N(t)$	Total population at time t	$N(t) \geq 0$	Individuals
2	$S(t)$	Number of individuals susceptible to DHF infection at time t	$S(t) \geq 0$	Individuals
3	$E(t)$	Number of individuals exposed to the dengue virus but not yet infectious at time t	$E(t) \geq 0$	Individuals
4	$I(t)$	Number of infected individuals capable of transmitting the dengue virus at time t	$I(t) \geq 0$	Individuals
5	$R(t)$	Number of individuals who have recovered and have temporary immunity against dengue infection at time t	$R(t) \geq 0$	Individuals

Table 2. List of parameters in the SEIR model.

No.	Parameter	Definition	Unit	Description
1	Λ	Population birth rate	Individuals/month	Adds individuals to the susceptible compartment S
2	μ	Natural mortality rate	$1/\text{month}$	Applies to all compartments
3	$\beta(T, P)$	Disease transmission rate influenced by temperature T and rainfall P	$1/\text{month}$	Determines the transition of individuals from S to E
4	σ	Transition rate from exposed individuals E to infected individuals I	$1/\text{month}$	Represents the transition of individuals from E to I
5	γ	Recovery rate of individuals from I to R	$1/\text{month}$	Represents the recovery rate of infected individuals
6	T	Average temperature	$^\circ\text{C}/\text{month}$	Climatic variable affecting β
7	P	Average rainfall	mm/month	Climatic variable affecting β
8	β_0	Baseline transmission rate	$1/\text{month}$	Obtained from the PSO parameter estimation process
9	β_1	Coefficient of the effect of temperature on the transmission rate	$1/(\text{month} \cdot {}^\circ\text{C})$	Obtained from the PSO parameter estimation process
10	β_2	Coefficient of the effect of rainfall on the transmission rate	$1/(\text{month} \cdot \text{mm})$	Obtained from the PSO parameter estimation process

In this study, temperature and rainfall data are incorporated using their original physical units, namely °C and mm/month, without normalization. This allows the coefficients β_1 and β_2 to directly represent the sensitivity of the transmission rate to changes in each physical unit of the climatic variables. In addition, the model assumes that climatic effects on disease transmission occur within the same monthly period. The time-lag effect between the accumulation of rainwater, the breeding cycle of Aedes aegypti mosquitoes, and the emergence of DHF cases is not explicitly modelled because the direct use of the effective transmission rate $\beta(T, P)$ allows climatic effects to be incorporated continuously and efficiently.

2.2. Variables and Parameters

The variables used in the DHF model with temperature and rainfall as climatic factors are presented in Table 1.

After defining the variables in the model, the next step is to determine the parameters used to represent interactions among populations and the rates of change in each compartment. These parameters include the transmission rate, recovery rate, mortality rate, and other parameters that contribute to the construction of the model. The parameters used to construct the model are presented in Table 2.

2.3. Model Analysis

Technically, because the transmission rate $\beta(T, P)$ varies with changes in temperature $T(t)$ and rainfall $P(t)$ over time, the SEIR model system in eq. (5) is nonautonomous. Therefore, to apply classical dynamic analysis techniques such as determining equilibrium points, calculating the basic reproduction number R_0, and analyzing local stability, the average temperature and rainfall values during the observation period, denoted by $\overline{T}$ and $\overline{P}$, are used. Meanwhile, the monthly dynamic climatic variables are fully incorporated into the numerical simulations and PSO parameter estimation.

2.3.1. Equilibrium Points

An equilibrium point represents a condition in which the populations in each compartment remain constant over time. Determining equilibrium points aims to understand the long-term behavior of disease transmission and how climatic factors such as temperature and rainfall affect the spread of DHF. The equilibrium condition is obtained when

$$\frac{dS}{dt} = \frac{dE}{dt} = \frac{dI}{dt} = \frac{dR}{dt} = 0. \tag{8}$$

2.3.2. Disease-Free Equilibrium Point

The disease-free equilibrium point (T_1) represents a theoretical condition in which no infected individuals are present in the population, with $I = 0$, $E = 0$, and $R = 0$. The existence of this equilibrium point does not automatically guarantee that the disease has been successfully controlled in practice. Disease control depends on the stability properties of the equilibrium point, which are determined by the value of the basic reproduction num-

ber R_0. If $R_0 < 1$, the disease-free equilibrium point is locally asymptotically stable, meaning that the number of infected cases will decrease toward zero over time and the disease can eventually disappear from the population. Conversely, if $R_0 > 1$, the equilibrium point becomes unstable, so the introduction of a small number of infected individuals may lead to disease transmission toward an endemic condition.

2.3.3. Endemic Equilibrium Point

If infected individuals ($I \neq 0$) remain in the population for a long period, meaning that the infection persists within the population, the system is said to be at an endemic equilibrium point.

2.3.4. Basic Reproduction Number

The basic reproduction number R_0 is an important indicator for determining whether an infection can spread or disappear from a population. The value of R_0 represents the average number of secondary infections generated by one infected individual in a population that is fully susceptible to the infection. A value of $R_0 > 1$ indicates that the disease is capable of spreading and persisting in the population, whereas $R_0 < 1$ indicates that the disease will eventually disappear from the population.

2.3.5. Stability Analysis of Equilibrium Points

Stability analysis is conducted to understand the behavior of the model system around an equilibrium point. After the equilibrium points are determined, stability analysis is performed for both equilibrium points. The first step is to linearize the system of differential equations around an equilibrium point (S, E, I, R). The result of this linearization process is then expressed in the form of the Jacobian matrix J. This approach allows the stability of each equilibrium point to be evaluated and provides information on whether the disease will spread or disappear from the population over time based on the model parameters.

2.4. Parameter Estimation

Parameter estimation was performed to obtain parameter values that best fit the observed data, so that the developed SEIR model can represent the dynamics of Dengue Hemorrhagic Fever (DHF) transmission more accurately. The estimated parameters include those affecting the transmission rate and the transition mechanisms between compartments, namely

$$\Theta = \{\beta_0, \beta_1, \beta_2, \sigma, \gamma, \mu\}, \tag{9}$$

with

$$\beta(T, P) = \beta_0 + \beta_1 T + \beta_2 P,$$

where T denotes the average temperature and P denotes the average rainfall at time t, σ is the incubation rate, γ is the recovery rate, and μ is the natural mortality rate.

The fitness function used in the estimation process is the Mean Absolute Percentage Error (MAPE) between the number of infected cases obtained from the simulation, $I_{\text{model}}(t;\Theta)$, and the observed number of infected cases, $I_{\text{data}}(t)$. The function is expressed as

$$\text{MAPE}(\Theta) = \frac{1}{n}\sum_{t=1}^{n}\frac{|I_{\text{data}}(t) - I_{\text{model}}(t;\Theta)|}{I_{\text{data}}(t)}. \tag{10}$$

A smaller MAPE value indicates a better fit between the model and the observed data. This study emphasizes the use of MAPE as the primary evaluation metric because it expresses prediction errors in percentage form, making them easier to interpret and suitable for evaluating the performance of the model in predicting dengue cases [23].

The stages of PSO for parameter estimation are described as follows.

1. Particle representation
   A particle is represented as a vector of length six. The elements of each particle are real-valued numbers used to represent the solution through the particle position and velocity.
2. Initialization of PSO parameters
   This stage is performed because the initial parameter settings determine the movement pattern of all particles during the solution search process. The PSO parameters consist of:
   - number of particles;
   - number of iterations;
   - inertia weight (w);
   - acceleration coefficients (c_1 and c_2); and
   - parameter bounds.

   Based on the incubation and recovery periods of DHF [24], the parameter ranges are defined as follows:

$$\begin{aligned}
\beta_0 &\in [0.1, 5],\\
\beta_1 &\in [0.001, 0.01],\\
\beta_2 &\in [0.00001, 0.0005],\\
\sigma &\in [3, 7.5],\\
\mu &\in [0.0008, 0.0011],\\
\gamma &\in [2, 4.5].
\end{aligned}$$

3. Initialization of the initial population
   (a) Determining the initial particle positions
   In this stage, each particle is placed at a random position within the search space at $t = 0$. The initial position is randomly generated within the specified parameter bounds:

$$x_{i,d}^{(0)} = x_{d,\min} + \text{rand}(0,1)\,(x_{d,\max} - x_{d,\min}), \tag{11}$$

   where $x_{i,d}^{(0)}$ is the position of the i-th particle in the d-th dimension at the initial iteration, $x_{d,\max}$ is the maximum value of the d-th dimension according to the upper bound of the corresponding parameter, and $x_{d,\min}$ is the minimum value of the d-th dimension according to the lower bound of the corresponding parameter.
   (b) Determining the initial particle velocities
   After the initial positions are determined, each particle is assigned an initial velocity $v_{i,d}^{(0)}$, which determines the direction and magnitude of particle movement in the subsequent iterations. Based on Shi and Eberhart (1998), the initial velocity is defined as

$$\begin{aligned}
v_{i,d}^{(0)} &= -v_{d,\max} + \text{rand}(0,1)\,[v_{d,\max} - (-v_{d,\max})],\\
v_{d,\max} &= 0.2\,(x_{d,\max} - x_{d,\min}),
\end{aligned} \tag{12}$$

where $v_{i,d}^{(0)}$ is the velocity of the i-th particle in the d-th dimension at the initial iteration, and $v_{d,\max}$ is the maximum velocity in the d-th dimension determined from the parameter bounds.

4. Fitness value calculation
   In this study, the fitness value is calculated through the following steps:
   (a) Substitute the parameter vector Θ in eq. (9) into the SEIR model in eq. (5) to calculate $I_{\text{model}}(t;\Theta)$ for each particle.
   (b) Calculate the value of $\beta(t)$ for each month.
   (c) Simulate the system of ordinary differential equations using the fourth-order Runge–Kutta method (RK4) with
   $$h = \frac{1}{\text{number of substeps per month}}.$$
   In the RK4 method, substeps are additional computational steps performed within a given time interval to obtain a more accurate approximation of the solution before determining the state variables at the next time point. In this study, 16 substeps per month are used.
   (d) Obtain the values of $I_{\text{model}}(t;\Theta)$ for $t = 0, \ldots, n$.
   (e) Calculate the MAPE between $I_{\text{model}}(t;\Theta)$ and $I_{\text{data}}(t)$ using eq. (10).
   (f) The resulting MAPE value is used as the initial personal best value of each particle and subsequently to determine the global best value. A smaller MAPE indicates a better parameter set.
5. Determining pbest and gbest
   The personal best, pbest, is determined from the first iteration until the maximum number of iterations is reached and may change at each iteration based on the particle fitness values. The pbest value is obtained from the fitness calculated using MAPE in the previous step. Meanwhile, gbest is the best value among all pbest values, corresponding to the smallest MAPE.
6. Determining the inertia weight
   The inertia weight is used in the particle velocity update and is adjusted until the maximum number of iterations is reached. This study uses the Linear Decreasing Inertia Weight (LDIW), given by
   $$w_k = w_{\max} - \frac{k}{k_{\max}}\left(w_{\max} - w_{\min}\right), \tag{13}$$
   where $w_{\max} = 0.9$, $w_{\min} = 0.4$, k is the current iteration, and $k_{\max}$ is the maximum number of iterations.
7. Particle velocity and position updates
   At this stage, the velocity of each particle is updated. All particles move toward the optimal position according to their velocities. The updated particle velocity is subsequently used to calculate the new particle position. The velocity update for each parameter is expressed as
   $$\begin{aligned} v_{i,d}^{(k+1)} = {} & w_k v_{i,d}^{(k)} + c_1 r_1 \left(\text{pbest}_{i,d} - x_{i,d}^{(k)}\right) \\ & + c_2 r_2 \left(\text{gbest}_d - x_{i,d}^{(k)}\right), \end{aligned} \tag{14}$$
   subject to
   $$v_{i,d}^{(k+1)} = \max\left\{\min\left[v_{i,d}^{(k+1)}, v_{d,\max}\right], -v_{d,\max}\right\},$$
   where $v_{i,d}^{(k+1)}$ is the velocity of the i-th particle in the d-th dimension at iteration $k+1$.
   After obtaining the updated velocity, the particle position for each parameter d is updated using
   $$x_{i,d}^{(k+1)} = x_{i,d}^{(k)} + v_{i,d}^{(k+1)}, \tag{15}$$
   subject to
   $$x_{i,d}^{(k+1)} = \max\left\{\min\left[x_{i,d}^{(k+1)}, x_{d,\max}\right], x_{d,\min}\right\},$$
   where $x_{i,d}^{(k+1)}$ is the position of the i-th particle in the d-th dimension at iteration $k+1$.
8. Re-evaluation and updating of pbest and gbest
   After obtaining the updated particle velocities and positions, the new positions are evaluated through the following steps:
   (a) Calculate the fitness value for each new position by simulating the SEIR model using RK4 and calculating the new MAPE value.
   (b) Update pbest if the new MAPE value is smaller than the previous value.
   (c) Update gbest if a new best pbest value is obtained.
   The evaluation process from the fitness calculation to the updating of pbest and gbest is repeated until the stopping criterion is satisfied.
9. Stopping criterion
   The PSO process terminates when the maximum number of iterations is reached. The final solution is the best particle stored in gbest at the end of the optimization process:
   $$\Theta^* = \text{gbest},$$
   which represents the parameter set producing the smallest MAPE value over all iterations.

2.5. Numerical Simulation

Numerical simulations were performed using the fourth-order Runge–Kutta method (RK4) with initial conditions determined from real data for Bandung City at the beginning of the observation period in January 2022. The total population of Bandung City was $N = 2{,}545{,}005$ individuals, based on data from Statistics Indonesia (BPS) of Bandung City. The initial value of the infected compartment was estimated from the initial monthly case data as $I(0) = 1{,}225$ individuals. The exposed compartment was set to $E(0) = 9{,}750$ individuals based on the incubation ratio approach, while $R(0) = 0$. The initial susceptible population was therefore calculated as

$$S(0) = N - E(0) - I(0) - R(0) = 2{,}534{,}030$$

individuals.

It should be noted that the monthly case records obtained from the Bandung City Health Office represent incidence data, namely newly reported cases during each month. In the mathematical model, the state variable $I(t)$ represents the number of actively infected individuals at time t. Therefore, the simulation was calibrated by matching the dynamics of $I(t)$ to the accumulated trend of the monthly reported cases.

3. Results and Discussion

3.1. Research Data

The data used in this study consist of secondary data covering the period from January 2022 to December 2023 (24 months), obtained from two official sources, namely monthly DHF incidence data and climatic variable data, including average temperature and rainfall. Monthly DHF case data were obtained directly from the Bandung City Health Office on 27 February 2026 in digital spreadsheet format (.xlsx), which had been officially approved by the Head of the Disease Prevention and Control Division of the Bandung City Health Office. Meanwhile, climatic variable data were obtained through the Open Data portal of Statistics Indonesia (BPS) of Bandung City. Before being used in the parameter estimation process using the PSO algorithm, all data were checked for completeness through a data cleaning process, and the DHF case data were processed using a 3-month Moving Average (MA) smoothing method to reduce short-term random fluctuations and emphasize the trend in disease transmission dynamics. The data used in this study are described as follows.

3.1.1. DHF Case Data

The DHF case data consist of the monthly number of confirmed DHF cases in Bandung City over a two-year period from 2022 to 2023. The data are presented in Table 3.

Table 3. DHF cases in Bandung City.

Year	Jan	Feb	Mar	Apr	May	Jun	Jul	Aug	Sep	Oct	Nov	Dec
2022	1225	738	457	428	445	416	357	311	226	201	198	203
2023	321	222	150	71	196	81	76	248	141	114	94	142

The DHF case data presented in tabular form were visualized graphically to facilitate analysis of the data pattern. The monthly distribution of DHF cases in Bandung City is presented in Figure 2.

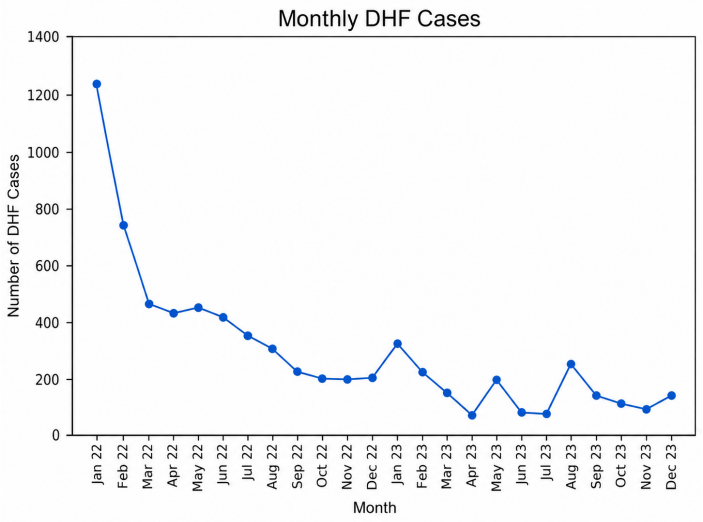

Figure 2. Monthly DHF cases in Bandung City.

Based on Figure 2, the data show considerable fluctuations with several substantial peaks. Therefore, a smoothing process using a 3-month Moving Average (MA) was applied to reduce short-term fluctuations and emphasize the underlying trend in the data. Mathematically, the 3-month MA is formulated as

$$MA_t = \frac{I_t + I_{t-1} + I_{t-2}}{3}, \tag{16}$$

where MA_t represents the moving average value at time t, and I_t represents the DHF case data at time t.

In the implementation, Python software was used to calculate the moving average. At the beginning of the observation period, the average was still calculated even when fewer than three observations were available. Therefore, the data for the first and second months were retained in the smoothing process, with the MA value calculated based on the number of observations available during the corresponding period. The smoothed DHF case data are presented in Figure 3.

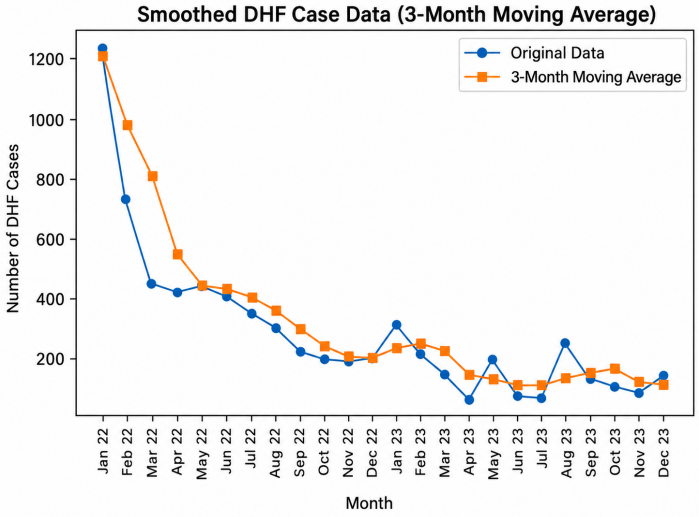

Figure 3. Smoothed DHF case data using the moving average method.

3.1.2. Climate Data

The climate data consist of monthly average air temperature and rainfall intensity obtained from Statistics Indonesia (BPS) of Bandung City. The climatic data are presented in Table 4.

3.1.3. Demographic Data

The estimated total population of Bandung City was used as the basis for determining the initial value of the susceptible population compartment. The total population was assumed to form a closed population and was subsequently divided into the SEIR model compartments, namely Susceptible (S), Exposed (E), Infected (I), and Recovered (R). The initial susceptible population was obtained by subtracting the initial numbers of exposed, infected, and recovered individuals from the total population.

3.2. Equilibrium Points and Basic Reproduction Number

Theoretically, because the climatic factors temperature $T(t)$ and rainfall $P(t)$ vary from month to month, the transmission rate $\beta(T, P)$ is a time-dependent function, causing the differential equation system of the model to be nonautonomous. Therefore, equilibrium analysis, calculation of the basic reproduction number R_0, and local stability analysis cannot be directly

Table 4. Climate data in Bandung City.

No.	Year	Month	Average Temperature (°C)	Rainfall (mm)
1	2022	January	23.3	59.5
2		February	23.5	117.1
3		March	24.1	238.9
4		April	23.3	336.2
5		May	23.9	146.9
6		June	22.8	150.6
7		July	23.1	98.5
8		August	23.3	29.9
9		September	23.3	182.2
10		October	23.2	366.7
11		November	23.4	307.2
12		December	23.3	277.7
13	2023	January	24.0	67.0
14		February	23.3	111.0
15		March	23.7	200.0
16		April	24.1	276.0
17		May	24.6	269.0
18		June	24.1	90.0
19		July	23.7	24.0
20		August	23.9	30.0
21		September	24.7	18.0
22		October	25.5	62.0
23		November	24.8	239.0
24		December	24.6	365.0

applied under these dynamic conditions. To perform qualitative analysis of the model, the system is simplified into an autonomous system by using the average temperature and rainfall values during the observation period, denoted by $\overline{T}$ and $\overline{P}$. Thus, the transmission rate in this subsection is represented by the constant average value

$$\beta(\overline{T},\overline{P}) = \beta_0 + \beta_1\overline{T} + \beta_2\overline{P}.$$

The average transmission rate $\beta(\overline{T},\overline{P})$ is subsequently used to determine the equilibrium points, construct the Next Generation Matrix (NGM), and formulate R_0.

3.2.1. Determination of Equilibrium Points

In the SEIR model, the equilibrium points are determined by setting

$$\frac{dS}{dt} = \frac{dE}{dt} = \frac{dI}{dt} = \frac{dR}{dt} = 0.$$

Therefore, the system in eq. (5) becomes

$$\Lambda - \beta(\overline{T},\overline{P})\frac{SI}{N} - \mu S = 0, \tag{17}$$

$$\beta(\overline{T},\overline{P})\frac{SI}{N} - (\sigma+\mu)E = 0, \tag{18}$$

$$\sigma E - (\gamma+\mu)I = 0, \tag{19}$$

and

$$\gamma I - \mu R = 0. \tag{20}$$

3.2.2. Disease-Free Equilibrium Point

To satisfy the disease-free equilibrium condition, let $I = 0$. It follows from eq. (19) and (20) that $E = 0$ and $R = 0$. From eq. (17), with $dS/dt = 0$, we obtain

$$S^* = \frac{\Lambda}{\mu}.$$

Using the constant demographic condition $\Lambda = \mu N$, it follows that

$$S^* = \frac{\mu N}{\mu} = N.$$

Therefore, the disease-free equilibrium point is given by

$$T_1 = (S,E,I,R) = \left(\frac{\Lambda}{\mu}, 0, 0, 0\right).$$

3.2.3. Endemic Equilibrium Point

The endemic equilibrium represents a condition in which the disease persists in the population, so that $I \neq 0$. Using the equilibrium conditions in eq. (17) to (20), the endemic equilibrium point is obtained as

$$T_2 = (S^*,E^*,I^*,R^*) = \left(\frac{N(\sigma+\mu)(\gamma+\mu)}{\sigma\beta(\overline{T},\overline{P})}, \frac{\gamma+\mu}{\sigma}I^*, I^*, \frac{\gamma}{\mu}I^*\right),$$

where

$$I^* = \frac{\Lambda\sigma}{(\sigma+\mu)(\gamma+\mu)} - \frac{\mu N}{\beta(\overline{T},\overline{P})}.$$

The value of I^* must be positive for the endemic equilibrium to exist biologically. This condition indicates that the disease can persist in the population when the effective transmission rate $\beta(\overline{T},\overline{P})$ is sufficiently large.

3.2.4. Basic Reproduction Number

The basic reproduction number R_0 is calculated using the Next Generation Matrix (NGM) approach [25]. In the mathematical model of DHF transmission, the infected compartments consist of the exposed population E and the infected population I. The corresponding differential equations are

$$\begin{aligned} \frac{dE}{dt} &= \beta(\overline{T},\overline{P})\frac{SI}{N} - (\sigma+\mu)E, \\ \frac{dI}{dt} &= \sigma E - (\gamma+\mu)I. \end{aligned} \tag{21}$$

Using F_i to represent the rate of new infections entering infected compartment i, and V_i to represent the net transfer of individuals into and out of infected compartment i due to disease progression, mortality, or recovery, we obtain

$$\begin{aligned} F_1 &= \beta(\overline{T},\overline{P})\frac{SI}{N}, \\ F_2 &= 0, \\ V_1 &= (\sigma+\mu)E, \\ V_2 &= -\sigma E + (\gamma+\mu)I. \end{aligned} \tag{22}$$

The Jacobian matrix associated with the new infection terms is

$$F = \begin{pmatrix} \frac{\partial F_1}{\partial E} & \frac{\partial F_1}{\partial I} \\ \frac{\partial F_2}{\partial E} & \frac{\partial F_2}{\partial I} \end{pmatrix} = \begin{pmatrix} 0 & \beta(\overline{T},\overline{P})\frac{S}{N} \\ 0 & 0 \end{pmatrix}.$$

At the disease-free equilibrium, $I = 0$ and

$$S = N = \frac{\Lambda}{\mu}.$$

Therefore,

$$F = \begin{pmatrix} 0 & \beta(\overline{T}, \overline{P}) \\ 0 & 0 \end{pmatrix}.$$

The Jacobian matrix associated with the transition terms is

$$V = \begin{pmatrix} \frac{\partial V_1}{\partial E} & \frac{\partial V_1}{\partial I} \\ \frac{\partial V_2}{\partial E} & \frac{\partial V_2}{\partial I} \end{pmatrix} = \begin{pmatrix} \sigma + \mu & 0 \\ -\sigma & \gamma + \mu \end{pmatrix}.$$

The inverse of V is

$$V^{-1} = \frac{1}{(\sigma + \mu)(\gamma + \mu)} \begin{pmatrix} \gamma + \mu & 0 \\ \sigma & \sigma + \mu \end{pmatrix},$$

or equivalently,

$$V^{-1} = \begin{pmatrix} \frac{1}{\sigma + \mu} & 0 \\ \frac{\sigma}{(\sigma + \mu)(\gamma + \mu)} & \frac{1}{\gamma + \mu} \end{pmatrix}.$$

The Next Generation Matrix is defined as

$$K = FV^{-1}.$$

Thus,

$$K = \begin{pmatrix} 0 & \beta(\overline{T}, \overline{P}) \\ 0 & 0 \end{pmatrix} \begin{pmatrix} \frac{1}{\sigma + \mu} & 0 \\ \frac{\sigma}{(\sigma + \mu)(\gamma + \mu)} & \frac{1}{\gamma + \mu} \end{pmatrix},$$

which gives

$$K = \begin{pmatrix} \frac{\sigma\beta(\overline{T}, \overline{P})}{(\sigma + \mu)(\gamma + \mu)} & \frac{\beta(\overline{T}, \overline{P})}{\gamma + \mu} \\ 0 & 0 \end{pmatrix}.$$

The basic reproduction number R_0 is determined from the spectral radius of the matrix K. The eigenvalues are obtained from the characteristic equation

$$\det(K - \lambda I) = 0.$$

Therefore,

$$\det\left[\begin{pmatrix} \frac{\sigma\beta(\overline{T}, \overline{P})}{(\sigma + \mu)(\gamma + \mu)} & \frac{\beta(\overline{T}, \overline{P})}{\gamma + \mu} \\ 0 & 0 \end{pmatrix} - \begin{pmatrix} \lambda & 0 \\ 0 & \lambda \end{pmatrix} \right] = 0,$$

so that

$$\det \begin{pmatrix} \frac{\sigma\beta(\overline{T}, \overline{P})}{(\sigma + \mu)(\gamma + \mu)} - \lambda & \frac{\beta(\overline{T}, \overline{P})}{\gamma + \mu} \\ 0 & -\lambda \end{pmatrix} = 0.$$

Hence,

$$\left(\frac{\sigma\beta(\overline{T}, \overline{P})}{(\sigma + \mu)(\gamma + \mu)} - \lambda \right)(-\lambda) = 0.$$

The eigenvalues are therefore

$$\lambda_1 = 0$$

and

$$\lambda_2 = \frac{\sigma\beta(\overline{T}, \overline{P})}{(\sigma + \mu)(\gamma + \mu)}.$$

Thus, the basic reproduction number is

$$R_0 = \frac{\sigma\beta(\overline{T}, \overline{P})}{(\sigma + \mu)(\gamma + \mu)}. \tag{23}$$

Here, $\beta(\overline{T}, \overline{P})$ represents the transmission rate under average climatic conditions. If $R_0 > 1$, the disease can persist in the population and an endemic condition may occur. Conversely, if $R_0 < 1$, the disease-free equilibrium is expected to be stable and the infection will gradually disappear from the population.

3.3. Local Stability Analysis

Local stability analysis is performed to determine the stability properties of the equilibrium points of the SEIR model by linearizing the system around each equilibrium point using the Jacobian matrix. The stability of the disease-free equilibrium is stated in Theorem 1.

Theorem 1. *The disease-free equilibrium point*

$$T_1 = \left(\frac{\Lambda}{\mu}, 0, 0, 0 \right)$$

is locally asymptotically stable if $R_0 < 1$ and unstable if $R_0 > 1$.

Proof. To determine the local stability of the disease-free equilibrium point, the system is linearized around the equilibrium point using the Jacobian matrix. The Jacobian matrix of the SEIR model is obtained by taking the partial derivatives with respect to the state variables (S, E, I, R), giving

$$J(S_0, E_0, I_0, R_0) = \begin{pmatrix} J_{11} & 0 & J_{13} & 0 \\ J_{21} & J_{22} & J_{23} & 0 \\ 0 & \sigma & J_{33} & 0 \\ 0 & 0 & \gamma & -\mu \end{pmatrix}, \tag{24}$$

where

$$J_{11} = -\beta(\overline{T}, \overline{P})\frac{I_0}{N} - \mu, \qquad J_{13} = -\beta(\overline{T}, \overline{P})\frac{S_0}{N},$$
$$J_{21} = \beta(\overline{T}, \overline{P})\frac{I_0}{N}, \qquad J_{22} = -(\sigma + \mu),$$
$$J_{23} = \beta(\overline{T}, \overline{P})\frac{S_0}{N}, \qquad J_{33} = -(\gamma + \mu).$$

To simplify the notation, define

$$u_1 = \sigma + \mu, \qquad u_2 = \gamma + \mu.$$

Thus, the Jacobian matrix in eq. (24) can be written as

$$J(S_0, E_0, I_0, R_0) = \begin{pmatrix} A_{11} & 0 & A_{13} & 0 \\ A_{21} & -u_1 & A_{23} & 0 \\ 0 & \sigma & -u_2 & 0 \\ 0 & 0 & \gamma & -\mu \end{pmatrix},$$

where

$$A_{11} = -\beta(\overline{T}, \overline{P})\frac{I_0}{N} - \mu, \qquad A_{13} = -\beta(\overline{T}, \overline{P})\frac{S_0}{N},$$
$$A_{21} = \beta(\overline{T}, \overline{P})\frac{I_0}{N}, \qquad A23 = \beta(\overline{T}, \overline{P})\frac{S_0}{N}.$$

At the disease-free equilibrium point

$$T_1 = \left(\frac{\Lambda}{\mu}, 0, 0, 0\right),$$

we have

$$S_0 = \frac{\Lambda}{\mu}, \qquad E_0 = I_0 = R_0 = 0, \qquad N = S_0 = \frac{\Lambda}{\mu}.$$

Substituting the disease-free equilibrium into eq. (24) gives

$$J(T_1) = \begin{pmatrix} -\mu & 0 & -\beta(\overline{T}, \overline{P}) & 0 \\ 0 & -u_1 & \beta(\overline{T}, \overline{P}) & 0 \\ 0 & \sigma & -u_2 & 0 \\ 0 & 0 & \gamma & -\mu \end{pmatrix}.$$

The eigenvalues are determined from

$$\det(J(T_1) - \lambda I) = 0.$$

Hence,

$$\begin{vmatrix} -\mu - \lambda & 0 & -\beta(\overline{T}, \overline{P}) & 0 \\ 0 & -u_1 - \lambda & \beta(\overline{T}, \overline{P}) & 0 \\ 0 & \sigma & -u_2 - \lambda & 0 \\ 0 & 0 & \gamma & -\mu - \lambda \end{vmatrix} = 0,$$

which yields

$$(-\mu - \lambda)^2 \left[\lambda^2 + (u_1 + u_2)\lambda + u_1 u_2 - \sigma\beta(\overline{T}, \overline{P})\right] = 0.$$

Therefore, the eigenvalues are

$$\lambda_1 = -\mu, \qquad \lambda_2 = -\mu,$$

and

$$\lambda_3 = \frac{-(u_1 + u_2) + \sqrt{(u_1 - u_2)^2 + 4\sigma\beta(\overline{T}, \overline{P})}}{2},$$

while

$$\lambda_4 = \frac{-(u_1 + u_2) - \sqrt{(u_1 - u_2)^2 + 4\sigma\beta(\overline{T}, \overline{P})}}{2}.$$

Using

$$R_0 = \frac{\sigma\beta(\overline{T}, \overline{P})}{(\sigma + \mu)(\gamma + \mu)},$$

the eigenvalues λ_3 and λ_4 can be expressed as

$$\lambda_3 = \frac{-(\sigma + \gamma + 2\mu) + \sqrt{(\sigma - \gamma)^2 + 4R_0(\sigma + \mu)(\gamma + \mu)}}{2},$$

and

$$\lambda_4 = \frac{-(\sigma + \gamma + 2\mu) - \sqrt{(\sigma - \gamma)^2 + 4R_0(\sigma + \mu)(\gamma + \mu)}}{2}.$$

Since the numerator of λ_4 is the sum of two negative terms, it follows that

$$\lambda_4 < 0.$$

For $\lambda_3 < 0$, the following condition must hold:

$$\sqrt{(\sigma - \gamma)^2 + 4R_0(\sigma + \mu)(\gamma + \mu)} < \sigma + \gamma + 2\mu.$$

Squaring both sides gives

$$(\sigma - \gamma)^2 + 4R_0(\sigma + \mu)(\gamma + \mu) < (\sigma + \gamma + 2\mu)^2.$$

Since

$$(\sigma + \gamma + 2\mu)^2 - (\sigma - \gamma)^2 = 4(\sigma + \mu)(\gamma + \mu),$$

the inequality is equivalent to

$$R_0 < 1.$$

Therefore, if $R_0 < 1$, then $\lambda_3 < 0$. Hence, all eigenvalues of the Jacobian matrix have negative real parts, and the disease-free equilibrium point T_1 is locally asymptotically stable. Conversely, if $R_0 > 1$, then $\lambda_3 > 0$, and the disease-free equilibrium point is unstable. □

After analyzing the local stability of the disease-free equilibrium point, the local stability of the endemic equilibrium point is considered to determine the condition under which the disease persists in the population. The stability of the endemic equilibrium is also determined from the eigenvalues of the Jacobian matrix evaluated at the equilibrium point and is stated in Theorem 2.

Theorem 2. *The endemic equilibrium point*

$$T_2 = (S^*, E^*, I^*, R^*) = \left(\frac{N(\sigma + \mu)(\gamma + \mu)}{\sigma\beta(\overline{T}, \overline{P})}, \frac{\gamma + \mu}{\sigma} I^*, I^*, \frac{\gamma}{\mu} I^*\right),$$

where

$$I^* = \frac{\Lambda\sigma}{(\sigma + \mu)(\gamma + \mu)} - \frac{\mu N}{\beta(\overline{T}, \overline{P})},$$

is locally asymptotically stable whenever it exists biologically, that is, when $I^* > 0$.

Proof. The Jacobian matrix in eq. (24) is evaluated at the endemic equilibrium point T_2, giving

$$J(T_2) = \begin{pmatrix} -\beta(\overline{T}, \overline{P})\frac{I^*}{N} - \mu & 0 & -\beta(\overline{T}, \overline{P})\frac{S^*}{N} & 0 \\ \beta(\overline{T}, \overline{P})\frac{I^*}{N} & -(\sigma + \mu) & \beta(\overline{T}, \overline{P})\frac{S^*}{N} & 0 \\ 0 & \sigma & -(\gamma + \mu) & 0 \\ 0 & 0 & \gamma & -\mu \end{pmatrix}.$$

Since

$$S^* = \frac{N(\sigma+\mu)(\gamma+\mu)}{\sigma\beta(\overline{T},\overline{P})},$$

we obtain

$$\beta(\overline{T},\overline{P})\frac{S^*}{N} = \frac{(\sigma+\mu)(\gamma+\mu)}{\sigma}.$$

Therefore,

$$J(T_2) = \begin{pmatrix} B_{11} & 0 & B_{13} & 0 \\ B_{21} & -(\sigma+\mu) & B_{23} & 0 \\ 0 & \sigma & -(\gamma+\mu) & 0 \\ 0 & 0 & \gamma & -\mu \end{pmatrix},$$

where

$$B_{11} = -\beta(\overline{T},\overline{P})\frac{I^*}{N} - \mu, \qquad B_{13} = -\frac{(\sigma+\mu)(\gamma+\mu)}{\sigma},$$
$$B_{21} = \beta(\overline{T},\overline{P})\frac{I^*}{N}, \qquad B_{23} = \frac{(\sigma+\mu)(\gamma+\mu)}{\sigma}.$$

Using

$$u_1 = \sigma+\mu, \qquad u_2 = \gamma+\mu,$$

the Jacobian matrix becomes

$$J(T_2) = \begin{pmatrix} -\beta(\overline{T},\overline{P})\frac{I^*}{N} - \mu & 0 & -\frac{u_1u_2}{\sigma} & 0 \\ \beta(\overline{T},\overline{P})\frac{I^*}{N} & -u_1 & \frac{u_1u_2}{\sigma} & 0 \\ 0 & \sigma & -u_2 & 0 \\ 0 & 0 & \gamma & -\mu \end{pmatrix}.$$

The eigenvalues are determined from

$$\det(J(T_2) - \lambda I) = 0.$$

Thus,

$$(-\mu-\lambda)\begin{vmatrix} -\beta(\overline{T},\overline{P})\frac{I^*}{N} - \mu - \lambda & 0 & -\frac{u_1u_2}{\sigma} \\ \beta(\overline{T},\overline{P})\frac{I^*}{N} & -u_1-\lambda & \frac{u_1u_2}{\sigma} \\ 0 & \sigma & -u_2-\lambda \end{vmatrix} = 0.$$

The characteristic equation can therefore be written as

$$(-\mu-\lambda)\left[\lambda^3 + A\lambda^2 + B\lambda + C\right] = 0,$$

where

$$A = \beta(\overline{T},\overline{P})\frac{I^*}{N} + \mu + u_1 + u_2,$$
$$B = \left(\beta(\overline{T},\overline{P})\frac{I^*}{N} + \mu\right)(u_1+u_2),$$

and

$$C = u_1u_2\beta(\overline{T},\overline{P})\frac{I^*}{N}.$$

One eigenvalue is

$$\lambda_1 = -\mu < 0,$$

because $\mu > 0$. The remaining eigenvalues λ_2, λ_3, and λ_4 are the roots of

$$\lambda^3 + A\lambda^2 + B\lambda + C = 0.$$

According to the Routh–Hurwitz criterion for a cubic polynomial, all roots have negative real parts if

$$A > 0, \qquad B > 0, \qquad C > 0, \qquad AB > C.$$

Because

$$\beta(\overline{T},\overline{P}) > 0, \qquad \mu > 0, \qquad u_1 > 0,$$
$$u_2 > 0, \qquad I^* > 0, \qquad N > 0,$$

it follows immediately that

$$A > 0, \qquad B > 0, \qquad C > 0.$$

Furthermore,

$$AB - C = \left(\beta(\overline{T},\overline{P})\frac{I^*}{N} + \mu + u_1 + u_2\right) \times \left(\beta(\overline{T},\overline{P})\frac{I^*}{N} + \mu\right)(u_1+u_2) - u_1u_2\beta(\overline{T},\overline{P})\frac{I^*}{N}.$$

Since all parameters are positive and $u_1+u_2 > 0$, the above expression is positive. Hence,

$$AB > C.$$

Therefore, all Routh–Hurwitz conditions are satisfied, implying that the roots λ_2, λ_3, and λ_4 have negative real parts. Together with $\lambda_1 = -\mu < 0$, this shows that

$$\mathrm{Re}(\lambda_i) < 0, \qquad i = 1,2,3,4.$$

Consequently, the endemic equilibrium point T_2 is locally asymptotically stable whenever it exists biologically. □

Biologically, this result indicates that when the system is near the endemic equilibrium point, small perturbations in the population do not permanently alter the long-term state of the system. The model solution will return to the endemic equilibrium, so the disease persists in the population at an endemic level.

3.4. *Parameter Estimation Using PSO*

Parameter estimation for the SEIR model was implemented using the Particle Swarm Optimization (PSO) algorithm in Python on the Google Colab platform. In this study, a reduced human population model was used in which the mosquito vector compartment was not explicitly included as a separate compartment. Instead, the effects of vector density and activity were incorporated directly through the effective transmission rate $\beta(T,P)$. The data used in the estimation process consisted of DHF cases, average temperature, and rainfall in Bandung City during 2022–2023. Each particle in the PSO algorithm represents the model parameter vector Θ defined in eq. (9). The initial position of each

particle was randomly generated within the predefined parameter bounds, and each particle was evaluated using the Mean Absolute Percentage Error (MAPE) objective function in eq. (10).

The MAPE value was obtained by first simulating the SEIR model using the fourth-order Runge–Kutta method (RK4). The simulation produced the number of infected individuals, which was then compared with the observed DHF case data to determine the MAPE value. A smaller MAPE value indicates that the corresponding parameter set provides a better representation of DHF transmission dynamics. Subsequently, the PSO algorithm updates the particle positions and velocities based on their personal best values (pbest) and the global best value (gbest) until the maximum number of iterations is reached. Through this process, the best model parameters corresponding to the lowest MAPE value are obtained.

Before the optimization process, the DHF case data were processed using a 3-month Moving Average (MA) method to reduce short-term fluctuations and make the underlying trend more apparent. The PSO algorithm was then applied to identify the parameter combination that minimized the MAPE value. To ensure the reproducibility of the experiment, the PSO algorithm settings were specified explicitly. The PSO parameter configuration used in this study is presented in Table 5.

Table 5. PSO parameter configuration.

PSO Parameter	Symbol	Value Used
Maximum inertia weight	$w_{\max}$	0.9
Minimum inertia weight	$w_{\min}$	0.4
Cognitive coefficient	c_1	2.0
Social coefficient	c_2	2.0
Number of particles	n_{particle}	60
Maximum number of iterations	$k_{\max}$	600
Velocity bound	v	$[-0.2, 0.2]$
Number of independent runs	–	10
Random seed	Seed	42
Model parameter bounds	Θ	$\beta_0 \in [0.1, 5]$, $\beta_1 \in [0.001, 0.01]$, $\beta_2 \in [0.00001, 0.0005]$, $\sigma \in [3, 7.5]$, $\mu \in [0.0008, 0.0011]$, $\gamma \in [2, 4.5]$

Since the PSO algorithm is stochastic, the consistency of the estimation results was evaluated using 10 independent runs. The evaluation results are presented in Table 6.

Table 6. Evaluation results from 10 independent parameter estimation runs.

Result	Value
Best MAPE	0.1740
Worst MAPE	–
Average MAPE	0.1791
Standard deviation	0.0048

Based on these results, the parameter combination corresponding to the best MAPE value was selected for numerical simulation and model evaluation. The relatively small standard deviation indicates that the PSO algorithm produced consistent parameter estimates across the independent runs.

The parameter estimation results produced the best values

$$\beta_0 = 3.5553, \quad \beta_1 = 0.0021, \quad \beta_2 = 0.0001,$$
$$\sigma = 7.5, \quad \mu = 0.0011, \quad \gamma = 3.6865,$$

with a MAPE value of 0.1740, or approximately 17.40%. Based on the estimated parameters β_0, β_1, and β_2, the transmission rate $\beta(T, P)$ varied according to the monthly climatic data in Bandung City. During the 2022–2023 observation period, the value of $\beta(T, P)$ ranged approximately from 3.6072 to 3.6435. The transmission rate remained nonnegative, $\beta(T, P) \geq 0$, over the entire range of observed temperature and rainfall data, thereby satisfying the biological requirement of the epidemiological model. The linear function was used as an initial approximation to capture the direct effects of temperature and rainfall on vector activity in a simple and computationally efficient manner.

The resulting MAPE value indicates that the model provides a reasonably good representation of the DHF case data in Bandung City. From a biological perspective, the estimated value $\sigma = 7.5$ corresponds to an average incubation period of approximately 4 days, while $\gamma = 3.6865$ corresponds to an average recovery period of approximately 8 days. In addition, the climate-dependent transmission parameters indicate that temperature and rainfall contribute to variations in the transmission pattern represented by the model. The application of the PSO algorithm therefore enabled the model to follow the trend of the smoothed DHF case data with predictive accuracy measured using MAPE. The smoothed data were used to reduce large fluctuations in the monthly observations so that the general transmission trend could be more clearly identified. Consequently, the numerical simulation results represent the trend of the smoothed data as an approximation of the dynamics of DHF transmission.

3.5. *Simulation and Model Evaluation*

Numerical simulations were performed to describe the dynamics of DHF transmission using the SEIR model with parameters obtained from the PSO estimation process. The simulations were conducted using the fourth-order Runge–Kutta method (RK4), incorporating the effects of temperature and rainfall on the disease transmission rate. The simulation results were then compared with the smoothed DHF case data to evaluate the extent to which the model followed the disease transmission pattern during the 2022–2023 observation period. The DHF case data generated by the SEIR model using the PSO-estimated parameters are presented in Figure 4.

The parameter estimation process and model simulation were evaluated against the DHF case data that had been smoothed using a 3-month Moving Average method. This step was performed to reduce short-term random fluctuations and emphasize the general trend of the disease dynamics. Based on this evaluation, the model produced a MAPE value of 0.1740, or 17.40%, relative to the smoothed data.

These results indicate that the developed SEIR model is reasonably capable of representing the main patterns and trends of DHF transmission dynamics, particularly for trend fitting, rather than serving as an absolute predictor of monthly case numbers. When evaluated directly against the original unsmoothed data,

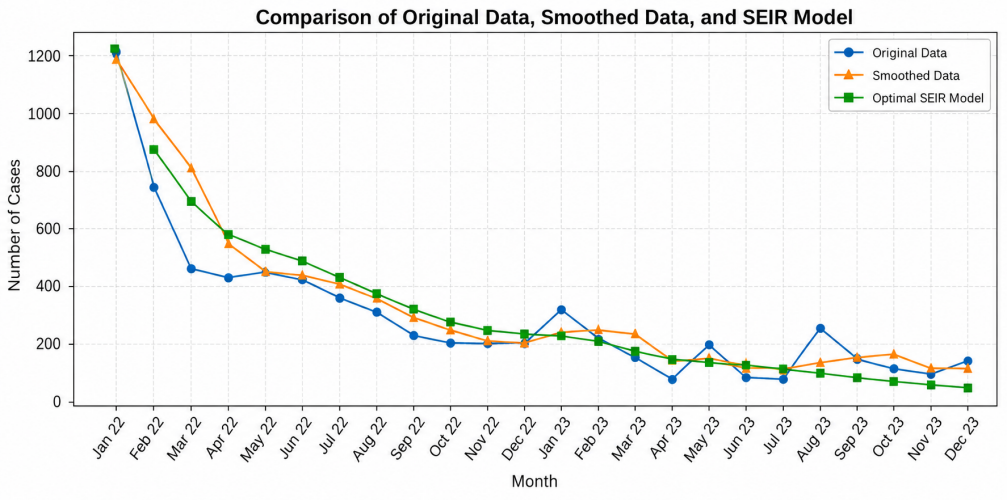

Figure 4. Comparison of DHF cases between the original data, smoothed data, and simulation results using the estimated parameters.

Table 7. Numerical results of parameter sensitivity analysis based on changes in MAPE.

No.	Parameter	MAPE -10%	MAPE $+10\%$	ΔMAPE -10%	ΔMAPE $+10\%$
1	β_0	0.587666	7.684147	0.413636	7.510117
2	β_1	0.178704	0.178245	0.004674	0.004215
3	β_2	0.176012	0.175898	0.001982	0.001868
4	σ	4.274759	118.050134	4.100729	117.876104
5	μ	0.175793	0.175714	0.001763	0.001684
6	γ	18.939629	104.423765	18.765599	104.249735

the model produced a MAPE value of 0.3544, or 35.44%. This difference reflects the substantial short-term fluctuations in the observed case data that may not be fully explained by macro-level climatic factors alone.

3.6. Sensitivity Analysis

3.6.1. Parameter Sensitivity Analysis with Respect to Model Goodness-of-Fit

Sensitivity analysis was conducted to evaluate the stability and sensitivity of the goodness-of-fit of the SEIR model to variations in the parameters obtained from PSO optimization using changes in MAPE, denoted by ΔMAPE, as the evaluation indicator. This analysis employed a local sensitivity analysis using the One-at-a-Time (OAT) approach. In this approach, one parameter was varied at a time while the remaining parameters were fixed at their optimal values obtained from PSO estimation. Each parameter, β_0, β_1, β_2, σ, μ, and γ, was varied by $\pm 10\%$ from its best estimated value. The model was then simulated again using the same initial conditions, and the MAPE value was recalculated by comparing the simulation results with the observed data. This method allows the effect of each parameter to be evaluated independently without interference from changes in other parameters [26].

The sensitivity level of each parameter was assessed based on the variation in the MAPE value after the parameter was perturbed. The optimal MAPE represents the MAPE value obtained from the best parameter set, while $\text{MAPE}_{-10\%}$ and $\text{MAPE}_{+10\%}$ represent the MAPE values obtained after decreasing and increasing the corresponding parameter by 10%, respectively. The changes in MAPE are calculated as

$$\Delta\text{MAPE}_{-10\%} = \text{MAPE}_{-10\%} - \text{MAPE}_{\text{optimal}},$$
$$\Delta\text{MAPE}_{+10\%} = \text{MAPE}_{+10\%} - \text{MAPE}_{\text{optimal}}.$$

A larger absolute value of ΔMAPE indicates a higher sensitivity of the corresponding parameter with respect to the goodness-of-fit of the model. The sensitivity analysis was performed locally by varying each parameter by $\pm 10\%$ from its best estimated value while keeping the other parameters constant. The numerical results of the parameter sensitivity analysis are presented in Table 7, which reports the MAPE values and the corresponding changes in MAPE for each parameter variation.

The changes in the simulation results caused by variations in each parameter are further illustrated in Figure 5 to show the influence of parameter perturbations on the goodness-of-fit of the model.

The results show that the recovery rate γ and the incubation or transition rate σ are the most sensitive parameters with respect to changes in model accuracy. A variation of $\pm 10\%$ in γ produces the largest increase in ΔMAPE compared with the other parameters. This indicates that the goodness-of-fit of the model is highly dependent on the precision of γ and σ. In contrast, the parameters β_1, β_2, and μ exhibit relatively low sensitivity with respect to MAPE, indicating that small variations in these parameters do not substantially affect the overall prediction error of the model.

3.6.2. Parameter Sensitivity Analysis with Respect to the Basic Reproduction Number

To further understand the epidemiological influence of the model parameters, sensitivity analysis was also performed with

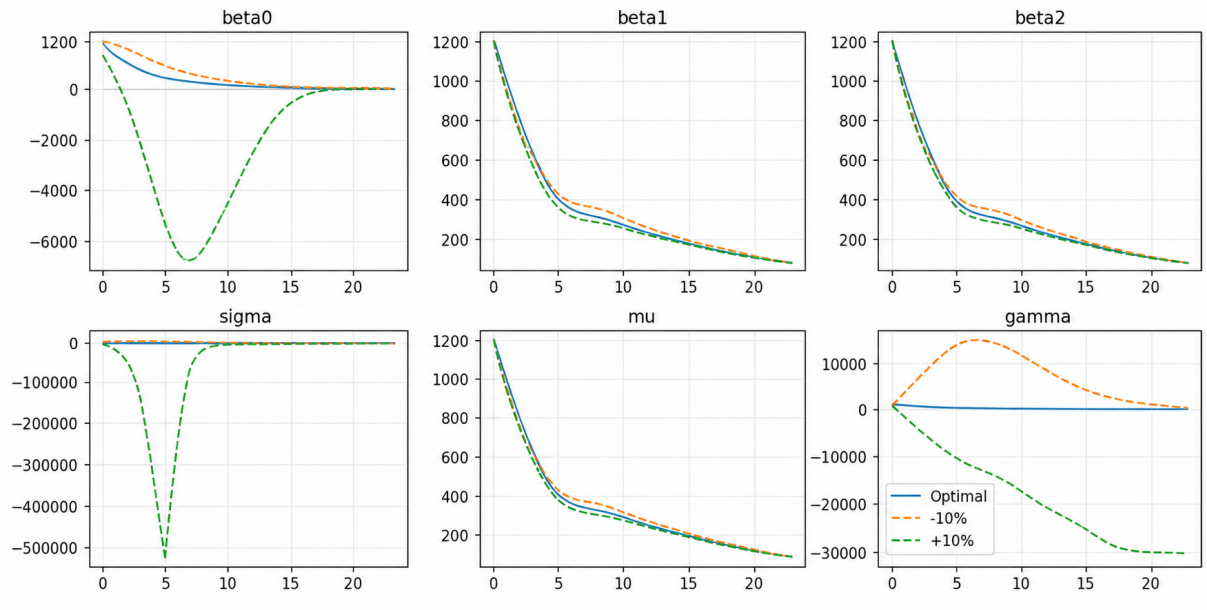

Figure 5. Parameter sensitivity analysis with respect to model goodness-of-fit.

Table 8. Sensitivity analysis of model parameters with respect to the basic reproduction number R_0.

No.	Parameter	Parameter Value	Sensitivity Index	Effect on R_0
1	β_0	3.5553	$+0.9724$	Dominant positive
2	β_1	0.0021	$+0.0135$	Positive
3	β_2	0.0001	$+0.0055$	Positive
4	σ	7.5	$+0.00015$	Positive (very small)
5	μ	0.0011	-0.00045	Negative (very small)
6	γ	3.6865	-0.9997	Dominant negative

respect to the basic reproduction number R_0 using the Normalized Forward Sensitivity Index. For a parameter p, the normalized sensitivity index is defined as

$$\Upsilon_p^{R_0} = \frac{\partial R_0}{\partial p}\frac{p}{R_0}.$$

Based on the best estimated parameter values, the normalized sensitivity indices of R_0 are presented in Table 8.

Based on the best estimated parameter values, the normalized sensitivity index $\Upsilon_{\beta_0}^{R_0} = +0.9724$ indicates that the baseline transmission rate β_0 has a strong positive proportional relationship with R_0. This means that a 10% increase in β_0 would result in an approximately 9.72% increase in R_0. Conversely, the recovery rate γ has a dominant negative sensitivity index of $\Upsilon_{\gamma}^{R_0} = -0.9997$. This indicates that a 10% increase in the recovery rate would decrease R_0 by approximately 9.99%.

The parameters σ and μ have sensitivity indices close to zero, indicating that small variations in these parameters have only a limited effect on R_0. Epidemiologically, these results suggest that reducing the baseline transmission rate β_0, for example through the elimination of mosquito breeding sites, and increasing the recovery rate γ through improved medical facilities and healthcare services are potentially the most effective strategies for reducing dengue transmission in Bandung City.

4. Conclusion

Based on the findings of this study, a mathematical model for the transmission of Dengue Hemorrhagic Fever (DHF) was formulated as a nonlinear SEIR system of differential equations by incorporating the effects of temperature and rainfall on the transmission rate. In this study, a reduced human population model was used in which the mosquito vector compartment, Aedes aegypti, was not explicitly included as a separate compartment. Instead, the effects of vector density and activity were incorporated directly through the effective transmission rate $\beta(T, P)$. Using the associated autonomous system under average climatic conditions, the model has two equilibrium points: the disease-free equilibrium $T_1 = \left(\frac{\Lambda}{\mu}, 0, 0, 0\right)$, which is locally asymptotically stable when $R_0 < 1$, and the endemic equilibrium $T_2 = \left(\frac{N(\sigma+\mu)(\gamma+\mu)}{\sigma\beta(\overline{T},\overline{P})}, \frac{\gamma+\mu}{\sigma}I^*, I^*, \frac{\gamma}{\mu}I^*\right)$, where $I^* = \frac{\Lambda\sigma}{(\sigma+\mu)(\gamma+\mu)} - \frac{\mu N}{\beta(\overline{T},\overline{P})}$, which exists and is locally asymptotically stable when $R_0 > 1$, with $R_0 = \frac{\sigma\beta(\overline{T},\overline{P})}{(\sigma+\mu)(\gamma+\mu)}$. Parameter estimation using the Particle Swarm Optimization (PSO) algorithm produced the optimal parameters for DHF case data in Bandung City during 2022–2023, namely $\beta_0 = 3.5553$, $\beta_1 = 0.0021$, $\beta_2 = 0.0001$, $\sigma = 7.5$, $\mu = 0.0011$, and $\gamma = 3.6865$. Based on the numerical simulation results, the model was able to follow the trend of the smoothed DHF case data with a MAPE value of 0.1740, or approximately 17.40%, indicating a relatively low fitting error. Thus, the developed model provides a reasonably good representation of DHF transmission dynamics while incorporating climatic factors.

Although the model is able to represent the dynamics of DHF cases reasonably well, the scope of this study is limited to a

direct transmission approach without explicitly considering the time lag between climatic changes and the biological response of the vector population. Future studies are recommended to incorporate Delay Differential Equations (DDE) or Distributed Lag Non-linear Models (DLNM) to better represent the extrinsic incubation period and delayed climatic effects on mosquito dynamics. In addition, other metaheuristic optimization algorithms, such as Genetic Algorithm or Simulated Annealing, may be included for comparative parameter estimation, while the analysis may be extended to spatial-temporal modelling to provide a more comprehensive representation of Dengue Hemorrhagic Fever transmission dynamics.

Author Contributions. **Sindi Meli Nur Afni**: Conceptualization, methodology, data collection, model implementation, formal analysis, visualization, writing—original draft preparation. **Khusnul Novianingsih**: Conceptualization, validation, supervision, writing—review and editing. **Ririn Sispiyati**: Methodology, validation, supervision, writing—review and editing.

Acknowledgement. The authors would like to thank all parties who contributed to this research and to the preparation of the manuscript. We also sincerely appreciate the editor and reviewers for their valuable comments and support in improving this work.

Funding. This research received no external funding.

Conflict of Interest. The authors declare no conflict of interest related to this article.

Data Availability. The data used in this study are available in the Results and Discussion section of this article.

References

[1] World Health Organization, "Dengue – global situation," 2024.
[2] N. Haider *et al.*, "Global dengue epidemic worsens with record 14 million cases and 9000 deaths reported in 2024," *International Journal of Infectious Diseases*, Sep 2025, doi:10.1016/j.ijid.2025.107940.
[3] Radio Republik Indonesia, "Kasus dbd kota bandung tertinggi di jabar," RRI.co.id.
[4] M. Aguiar *et al.*, "Mathematical models for dengue fever epidemiology: A 10-year systematic review," *Physics of Life Reviews*, Mar 2022, doi:10.1016/j.plrev.2022.02.001.
[5] A. Osi and N. Ghaffarzadegan, "Parameter estimation in behavioral epidemic models with endogenous societal risk-response," *PLoS Computational Biology*, vol. 20, no. 3, Mar 2024, doi:10.1371/journal.pcbi.1011992.
[6] K. Gopal, L. S. Lee, and H. V. Seow, "Parameter estimation of compartmental epidemiological model using harmony search algorithm and its variants," *Applied Sciences*, vol. 11, no. 3, pp. 1–25, Feb 2021, doi:10.3390/app11031138.
[7] O. Septiriani and M. K. Sudaryo, "Pengaruh iklim terhadap kasus dengue di kota bandung: 2011–2020," *Kesmas Indonesia*, vol. 14, no. 1, p. 75, Jan 2022, doi:10.20884/1.ki.2022.14.1.5240.
[8] Y. Cheng, R. Cheng, T. Xu, X. Tan, Y. Bai, and J. Yang, "Integrating meteorological data and hybrid intelligent models for dengue fever prediction," *BMC Public Health*, vol. 25, no. 1, p. 1516, Apr 2025, doi:10.1186/s12889-025-22375-2.
[9] N. M. H. Nik Abdull Halim, N. Che Dom, R. Dapari, H. Salim, and N. Precha, "A systematic review and meta-analysis of the effects of temperature on the development and survival of the aedes mosquito," *Frontiers in Public Health*, vol. 10, Dec 2022, doi:10.3389/fpubh.2022.1074028.
[10] M. H. Zahid *et al.*, "The biting rate of aedes aegypti and its variability: A systematic review (1970–2022)," *PLoS Neglected Tropical Diseases*, vol. 17, no. 8, p. e0010831, Aug 2023, doi:10.1371/journal.pntd.0010831.
[11] Y. Li, Q. Dou, Y. Lu, H. Xiang, X. Yu, and S. Liu, "Effects of ambient temperature and precipitation on the risk of dengue fever: A systematic review and updated meta-analysis," *Environmental Research*, vol. 191, p. 110043, Dec 2020, doi:10.1016/j.envres.2020.110043.
[12] E. Buckingham-Jeffery, V. Isham, and T. House, "Gaussian process approximations for fast inference from infectious disease data," *Mathematical Biosciences*, vol. 301, pp. 111–120, Jul 2018, doi:10.1016/j.mbs.2018.02.003.
[13] T. Kypraios, P. Neal, and D. Prangle, "A tutorial introduction to bayesian inference for stochastic epidemic models using approximate bayesian computation," *Mathematical Biosciences*, vol. 287, pp. 42–53, May 2017, doi:10.1016/j.mbs.2016.07.001.
[14] T. Ganyani, C. Faes, and N. Hens, "Simulation and analysis methods for stochastic compartmental epidemic models," *Annual Review of Statistics and Its Application*, vol. 8, no. 1, pp. 69–88, Mar 2021, doi:10.1146/annurev-statistics-061120-034438.
[15] R. Bidhendi Yarandi, M. A. Mansournia, H. Zeraati, and K. Mohammad, "An intuitive framework for bayesian posterior simulation methods," *Global Epidemiology*, vol. 3, p. 100060, Nov 2021, doi:10.1016/j.gloepi.2021.100060.
[16] S. Kim, A. C. Hooker, Y. Shi, G. H. J. Kim, and W. K. Wong, "Metaheuristics for pharmacometrics," *CPT: Pharmacometrics & Systems Pharmacology*, vol. 10, no. 11, pp. 1297–1309, Nov 2021, doi:10.1002/psp4.12714.
[17] W. Nur and Z. Nur, "Estimasi parameter model sir dengan algoritma genetik," *JOMTA Journal of Mathematics: Theory and Applications*, vol. 1, no. 2, 2019.
[18] Windarto, M. A. Khan, and Fatmawati, "Parameter estimation and fractional derivatives of dengue transmission model," *AIMS Mathematics*, vol. 5, no. 3, pp. 2758–2779, 2020, doi:10.3934/math.2020178.
[19] F. Pace, A. Santilano, and A. Godio, "A review of geophysical modeling based on particle swarm optimization," *Surveys in Geophysics*, vol. 42, no. 3, pp. 505–549, May 2021, doi:10.1007/s10712-021-09638-4.
[20] A. Chamnan, P. Pongsumpun, I. M. Tang, and N. Wongvanich, "Optimal control of dengue transmission with vaccination," *Mathematics*, vol. 9, no. 15, p. 1833, Aug 2021, doi:10.3390/math9151833.
[21] H. M. Yang, M. L. G. Macoris, K. C. Galvani, M. T. M. Andrighetti, and D. M. V. Wanderley, "Assessing the effects of temperature on the population of Aedes aegypti, the vector of dengue," *Epidemiology and Infection*, vol. 137, no. 8, pp. 1188–1202, Aug 2009, doi:10.1017/S0950268809002040.
[22] Y. L. Hii, J. Rocklöv, N. Ng, C. S. Tang, F. Y. Pang, and R. Sauerborn, "Climate variability and increase in intensity and magnitude of dengue incidence in singapore," *Global Health Action*, vol. 2, no. 1, p. 2036, Nov 2009, doi:10.3402/gha.v2i0.2036.
[23] D. Chicco, M. J. Warrens, and G. Jurman, "The coefficient of determination r-squared is more informative than smape, mae, mape, mse and rmse in regression analysis evaluation," *PeerJ Computer Science*, vol. 7, p. e623, Jul 2021, doi:10.7717/peerj-cs.623.
[24] World Health Organization, "Dengue and severe dengue," 2025.
[25] P. van den Driessche and J. Watmough, "Reproduction numbers and subthreshold endemic equilibria for compartmental models of disease transmission," *Mathematical Biosciences*, vol. 180, no. 1–2, pp. 29–48, Nov 2002, doi:10.1016/S0025-5564(02)00108-6.
[26] X. Lu and E. Borgonovo, "Global sensitivity analysis in epidemiological modeling," *European Journal of Operational Research*, vol. 304, no. 1, pp. 9–24, Jan 2023, doi:10.1016/j.ejor.2021.11.018.